On the Origin of the Trojan Asteroids: Effects of Jupiter's Mass Accretion and Radial Migration

Heather J. Fleming and Douglas P. Hamilton

Astronomy Department, University of Maryland, College Park, Maryland 20742-2421
E-mail: hamilton@astro.umd.edu

We present analytic and numerical results which illustrate the effects of Jupiter's accretion of nebular gas and the planet's radial migration on its Trojan companions. Initially, we approximate the system by the planar circular restricted three-body problem and assume small Trojan libration amplitudes. Employing an adiabatic invariant calculation, we show that Jupiter's 30-fold growth from a $10 M_\oplus$ core to its present mass causes the libration amplitudes of Trojan asteroids to shrink by a factor of about 2.5 to ∼40% of their original size. The calculation also shows that Jupiter's radial migration has comparatively little effect on the Trojans; inward migration from 6.2 to 5.2 AU causes an increase in Trojan libration amplitudes of ∼4%. In each case, the area enclosed by small tadpole orbits, if made dimensionless by using Jupiter's semimajor axis, is approximately conserved. Similar adiabatic invariant calculations for inclined and eccentric Trojans show that Jupiter's mass growth leaves the asteroids' eccentricities and inclinations essentially unchanged, while 1 AU of inward migration causes an increase in both of these quantities by ∼4%. Numerical integrations confirm and extend these analytic results. We demonstrate that our predictions remain valid for Trojans with small libration amplitudes even when the asteroids have low, but nonzero, eccentricities and inclinations and/or Jupiter has an eccentricity similar to its present value. The integrations also show that Trojans with large libration amplitudes, including horseshoe orbits, are even more strongly affected by Jupiter's mass growth and radial migration than simple scaling from our analytic results would suggest. Further, the numerical runs demonstrate that Jupiter's predicted mass growth is sufficient to cause the capture of asteroids initially on horseshoe orbits into stable tadpole orbits. Thus, if Jupiter captured most of its Trojan companions before or while it accreted gas, as seems probable, then Jupiter's growth played a significant role in stabilizing Trojan objects by systematically driving them to lower libration amplitudes. © 2000 Academic Press

Key Words: asteroids, dynamics; celestial mechanics; Jupiter; origin, Solar System; resonances.

1. INTRODUCTION

The Trojans are a distant group of asteroids dynamically linked to Jupiter by a 1:1 mean motion resonance which causes them to librate about stable Lagrangian equilibrium points lo-cated 60° in front of (L4) and behind (L5) Jupiter along its orbit. Because Trojans orbit far from the Sun and also have low albedos, they suffer from a low discovery rate and hence are underrepresented among numbered asteroids. Extrapolating from the identified Trojan objects, Shoemaker *et al.* (1989) estimate that the total Trojan population contains nearly half as many asteroids as the main belt. The large number of Trojans and their strong dynamical connection to Jupiter make determining their origins an important goal; by understanding the early history of the Trojans, we may also gain insight into Jupiter's formation and early evolution.

Clues about the origins of the Trojan asteroids may be found in their current physical and orbital properties, which include the overlapping signatures of mechanisms which captured them into librating orbits, as well as processes which have contributed to the population's evolution over time. Some distinctive characteristics of the current Trojan asteroids include a small mean eccentricity of ∼0.06, a small mean libration amplitude of ∼29°, and a large mean inclination of ∼18° (Shoemaker *et al.* 1989, Levison *et al.* 1997). Also, nearly twice as many asteroids have been observed librating about the L4 point as about the L5 point. This, however, may simply be the result of observational selection effects (Shoemaker *et al.* 1989).

There are many competing theories for the origin and evolution of the Trojan asteroids. It has been suggested that the Trojans may have originally been comets (Rabe 1972) or near-Jupiter planetesimals (e.g., Shoemaker *et al.* 1989, Kary and Lissauer 1995). A number of mechanisms have been considered for capturing these objects into Trojan orbits, including collisions between objects, drag forces, and mass accretion by Jupiter. Shoemaker *et al.* (1989) theorized that collisional emplacement of fragments of near-Jupiter planetesimals during the dispersion of the planetesimal swarm may have provided most of the Trojan objects. More recently, numerical modeling of the collisional evolution of the Trojan population (Marzari *et al.* 1997) has shown that collisions are largely responsible for shaping the current size distribution of the smaller Trojans, as well as having caused the escape of some of the Trojan objects into chaotic orbits. Long-term numerical integrations by Levison *et al.* (1997) have also shown that the Trojan population is dynamically

TABLE I
Effects of Jovian Accretion and Migration on Trojan Libration Amplitudes

	If planetary mass increased	If inward radial migration
Rabe (1954)	A increases	X
Horedt (1974a,b, 1984)	A unaffected	X
Yoder (1979)	A decreases	A decreases
This work	A decreases	A increases

unstable and that dynamical diffusion has contributed and continues to contribute to the loss of Trojan objects. This diffusion would have been enhanced in the early solar system if Jupiter and Saturn were closer together than they are currently (Gomes 1998).

Various types of drag forces acting on Jupiter and/or the Trojan precursors have also been examined. Kary and Lissauer (1995) showed numerically that Solar nebular gas drag could cause planetesimals to be captured into 1:1 resonance with a protoplanet. Interestingly, they found that such capture is rare for planets on circular orbits, but quite common for planets with appreciable eccentricities. Gas drag may also have played a significant role in evolving the Trojan population into its present form, provided that the Trojan precursors were captured before the dispersion of the solar nebula (Peale 1993). Yoder (1979) looked at the effects of dynamical friction during Jupiter's dispersal of the planetesimal swarm, which caused a slight inward migration of Jupiter. He argued that this migration would cause a decrease in the libration amplitudes of Jupiter's Trojan companions (see, however, Table I).

The possibility that a change in Jupiter's mass could be responsible for the capture of the Trojan asteroids was investigated by Rabe (1954), who argued analytically that a decrease in Jupiter's mass could cause its satellites to move onto Trojan orbits. More recently, Marzari and Scholl (1998) showed numerically that an increase in Jupiter's mass could cause the capture of planetesimals into librating orbits. They used a proto-Jupiter on a "best guess" orbit growing simultaneously with Saturn over a period of 10^4 or 10^5 years and found that a large fraction of the planetesimals initially on horseshoe orbits and a small percentage of those initially orbiting near the 1:1 resonance were captured into tadpole orbits.

Past changes in Jupiter's mass have also long been considered a potentially significant evolutionary mechanism for creating the current distribution of Trojan asteroids; however, attempts to predict the exact form of the effects of Jupiter's growth on the Trojans have thus far been contradictory. For an increase in Jupiter's mass, Rabe (1954) theorized that the Trojan libration amplitudes would increase, Horedt (1974a,b, 1984) argued that they would not be appreciably affected, and Yoder (1979) predicted that they would decrease (Table I).

In this paper, we focus on the changes which Jupiter underwent early in its history. We investigate the significance of

Jupiter's mass growth and radial migration as Trojan capture mechanisms and especially as mechanisms for evolving the Trojan population. We focus on these two processes in isolation in order to fully characterize their behavior. Other potentially important processes including gas drag, the gravity of other planets and/or protoplanets, and collisions among Trojans are not considered here, because models which include all of these effects would have a large number of poorly determined free parameters. For example, with gas drag, what is the gas density as a function of distance from the Sun? When and exactly how does Jupiter form a gap in the gas distribution? How sensitive are Trojan asteroids to different gas drag models? These questions are important and need to be studied in depth. There are many open questions like these in the full Trojan formation problem, probably more than can be addressed in a single paper. Accordingly, we have chosen to study individual processes first for later incorporation into a more general model. A strong advantage to this approach is that investigating individual processes in detail will ultimately lead to a deeper physical understanding of results from more complicated models.

Adopting this approach, we first present consistent analytic and numerical results which show the effects of Jupiter's growth and radial migration on its Trojan companions in the limit of a slowly changing Jupiter, thus settling the previous controversy. We then explore the working of these mechanisms for a wide range of time scales, initial Trojan libration amplitudes, Jupiter eccentricities, and asteroid eccentricities and inclinations.

2. ANALYTIC RESULTS

2.1. Libration Amplitude

Consider the planar circular restricted three-body problem, in which two massive bodies move about each other in circular orbits due to their mutual gravitation and a third body of infinitesimal mass moves in the orbital plane of the two massive objects. This system admits five equilibrium points where a test particle can have zero velocity and zero acceleration in the frame which corotates with the primary masses about their common center of mass (Danby 1988). Three of these points lie along the line through the two primaries and are unstable. The other two, L4 and L5, lie at the tips of the equilateral triangles whose bases are the line connecting the primary masses (see Fig. 1). These are called the triangular Lagrangian equilibrium points and are stable to small oscillations so long as the mass ratio of the primaries, $\mu = M_2/(M_1 + M_2)$ (where M_1 and M_2 are the larger and smaller of the primary masses, respectively), satisfies $\mu \lesssim 0.0385$ (Murray and Dermott 1999). This condition is met for all Sun–planet and planet–moon pairs in the Solar System, with the exception of Pluto and Charon.

The planar circular restricted three-body problem is a reasonable approximation for the system consisting of the Sun, Jupiter, and a Trojan asteroid, since the asteroid's mass is insignificant in comparison to either Jupiter or the Sun, and Jupiter's eccentricity is relatively small ($\sim$0.0483 currently). If we make
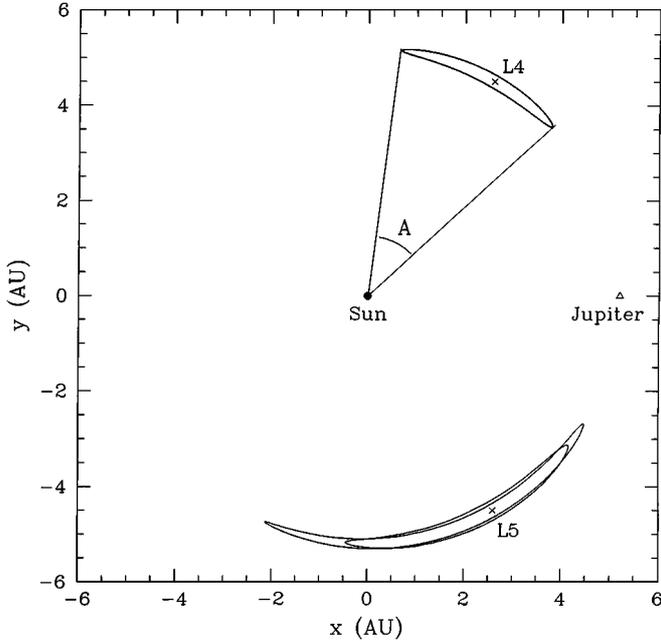
FIG. 1. Three sample Trojan asteroid orbits are plotted in the frame which corotates with Jupiter about the center of mass of the Sun–Jupiter system. The L4 (leading) and L5 (trailing) Lagrangian equilibrium points are each indicated by the symbol ×. The orbits shown, which enclose either the L4 or the L5 point, but not both, are called tadpoles due to the shape of their librations. The tadpole around the L4 point was integrated with Jupiter at twice its present mass, which makes it wider and thus easier to view. The libration amplitude, $A \simeq 40°$, is indicated for this orbit. The two tadpoles about the L5 point are the initial (long, thin tadpole with $A \simeq 85°$) and final (short, fat tadpole with $A \simeq 60°$) orbits for a Trojan as Jupiter's mass grows slowly from one-half to twice its current value. The tadpole both shortens and widens as Jupiter's mass increases.

the further approximations that the Trojan's oscillations about its equilibrium position are small and that the asteroid is on a nearly circular orbit, then, noting that

$$\mu = \frac{M_J}{M_S + M_J} \approx 0.001 \ll 1, \tag{1}$$

where M_S is the mass of the Sun and M_J is the mass of Jupiter, the motion of the asteroid is well approximated by the equation

$$\ddot{\phi}_* + \left(\frac{27}{4}\right)\mu n_J^2 \phi_* = 0 \tag{2}$$

(Brown and Shook 1964). Here an overdot signifies differentiation with respect to time, $\phi_* = \phi - \phi_{eq}$, where ϕ is the angular position of the asteroid and ϕ_{eq} is the angular position of the Lagrangian equilibrium point about which the asteroid librates, both measured with respect to Jupiter. Finally, Jupiter's mean motion is given by

$$n_J = \left[\frac{G(M_S + M_J)}{a_J^3}\right]^{1/2}, \tag{3}$$

where a_J is Jupiter's semimajor axis and G is the gravitational constant. The observed librational motions of the Trojan asteroids are well described by the solution of Eq. (2),

$$\phi_* = \frac{A}{2}\cos(\omega t + B), \tag{4}$$

where

$$\omega^2 = \frac{27}{4}\mu n_J^2, \tag{5}$$

t is time, and A and B are constants. Note that $A/2$ is the amplitude of the ϕ oscillations. The libration amplitude, A, is defined to be the total angular extent of these oscillations (see Fig. 1). Equivalently, the system can be described by the Hamiltonian

$$H = \frac{1}{2}a_J^2\dot{\phi}_*^2 + \frac{1}{2}\omega^2 a_J^2\phi_*^2, \tag{6}$$

which has units of energy over mass. We use this rather than the full Hamiltonian with units of energy since the Trojan's mass is ignored in deriving Eq. (2). The canonical variables for this Hamiltonian are $q = a_J\phi_*$ and $p = a_J\dot{\phi}_*$, so that $\frac{\partial H}{\partial p} = \dot{q}$, and $\frac{\partial H}{\partial q} = -\dot{p}$ reproduces the equation of motion (Eq. 2).

When changes are made to external parameters governing the system (e.g., mass growth of Jupiter or the Sun or an external torque on either of them), the Hamiltonian is no longer conserved. However, if these changes are slow enough, relatively smooth, and not in resonance with the system, then it can be shown that the action, $J = \int p\, dq$, is approximately conserved (Landau and Lifschitz 1960, Arnold 1978, Corben and Stehle 1957). Such changes are called adiabatic changes and J is an adiabatic invariant. To have physical relevance, the adiabatic invariant J must be derived from a Hamiltonian which gives the correct energy of the system (to within a constant). Using the expressions for p, q, and ϕ_* above, we determine the action for the three-body system:

$$J_{3body} = \int a_J^2\dot{\phi}_*\, d\phi_* = \int_0^{2\pi/\omega} a_J^2 A^2\omega^2 \sin^2(\omega t + B)\, dt$$

$$= \frac{\pi}{4}\sqrt{\frac{27G}{4}} A^2 M_J^{1/2} a_J^{1/2} = \text{constant}, \tag{7}$$

where we have evaluated the integral by using the adiabatic approximation that a_J, A, and ω are constant over one libration period.

The conservation of the action can be written in the useful form

$$\frac{A_f}{A_i} = \left(\frac{M_{Jf}}{M_{Ji}}\right)^{-1/4}\left(\frac{a_{Jf}}{a_{Ji}}\right)^{-1/4}, \tag{8}$$

where the subscripts i and f indicate the initial and final values of the variables, respectively.

For radial migration of Jupiter, we can find the resulting change in the Trojan's libration amplitude directly from Eq. (8); since changing a_J has no effect on M_J, the factor $(M_{Jf}/M_{Ji})^{-1/4}$ is equal to 1. Then, for a physically reasonable inward radial migration of Jupiter from approximately 6.2 to 5.2 AU (see Section 4), Eq. (8) predicts an increase in the Trojan's libration amplitude of only ~4%.

Determining the effects of Jupiter's mass growth on the Trojan's libration amplitude is a bit more subtle, since increasing M_J may affect a_J as well as A. The problem of how the semimajor axis of an orbit adjusts to mass accretion onto one member of a binary system has a long history, which goes back at least to Strömgen (1903), who considered what effect mass accretion by the Earth would have on the orbit of the Moon. Jeans (1961) provides a nice derivation of the effects of mass loss from a binary system via stellar radiation or stellar winds. For both of these cases, mass gain (or loss) is isotropic in the frame in which the affected body is at rest. With the isotropic assumption, Jeans (1961) shows that

$$(M_S + M_J)a_J = \text{constant.} \qquad (9)$$

Although the accretion of solar nebular gas by Jupiter may not have been perfectly isotropic, this is a reasonable approximation. We will return to investigate anisotropic mass changes shortly. Equation (9) predicts that if the mass of either Jupiter or the Sun were slowly decreased, Jupiter's orbit would drift outward. This effect is well known (e.g., Horedt 1984) and was observed recently in numerical simulations by Duncan and Lissauer (1998), in which the orbits of the outer planets were seen to expand as the mass of the Sun was decreased to a small fraction of its original value. Similarly, if either Jupiter or the Sun slowly accretes mass, Jupiter's semimajor axis will decrease. Note that Eq. (9) implies that adding a Jovian mass of material to either Jupiter or the Sun produces the same change in the semimajor axis of the system.

Returning to our discussion of the effects of Jupiter's mass growth on its Trojan companions, we see from Eq. (9) that if the mass of Jupiter is changed adiabatically and isotropically, the semimajor axis of Jupiter's orbit will be altered according to

$$\frac{a_{Jf}}{a_{Ji}} = \frac{M_S + M_{Ji}}{M_S + M_{Jf}}. \qquad (10)$$

Substituting this into Eq. (8), we obtain the full effect which altering M_J has on the Trojan's libration amplitude:

$$\frac{A_f}{A_i} = \left(\frac{M_{Jf}}{M_{Ji}}\right)^{-1/4} \left(\frac{M_S + M_{Jf}}{M_S + M_{Ji}}\right)^{1/4}. \qquad (11)$$

Since $M_J \ll M_S$, the second term in parentheses is very nearly equal to 1, and the change in A is given sufficiently accurately by Eq. (8) if we simply take $(a_{Jf}/a_{Ji})^{-1/4} = 1$. We can generalize this result to anisotropic forms of mass accretion if we know how

much radial migration results from the accretion. For example, if accretion of gas exerted torques on Jupiter which forced a 1-AU shift in its distance from the Sun, then the first term on the right-hand side of Eq. (8) still dominates the second. In fact, the effect of Jupiter's radial migration is comparable to its ~30-fold growth in mass only if the planet moves inward by a factor of ~30, e.g., from 150 to 5 AU.

Thus, for all reasonable mass accretion and radial migration scenarios, accretion dominates, and we find that the growth of Jupiter from a ~$10M_\oplus$ core to its present mass of ~$320M_\oplus$ causes A to decrease by a factor of ~2.5 to ~40% of its original value. If librating Trojan asteroids were already present when Jupiter was a $10M_\oplus$ core, then their orbits were substantially stabilized by Jupiter's growth.

There has been some significant confusion in the literature about the effects of Jupiter's mass growth on the libration amplitudes of its Trojan companions (see Table I). Our analytic result for the effects of Jovian mass growth disagrees with the findings of Rabe (1954) and Horedt (1974a,b, 1984), but agrees exactly, in both direction and magnitude, with the conclusions of Yoder (1979). Our prediction for the effects of Jupiter's radial migration, however, disagrees with Yoder's 1979 result (see Table I). Statements in Yoder *et al.* (1983) about the tidal evolution of the saturnian satellites Janus and Epimetheus, however, are inconsistent with Yoder's 1979 calculations, but agree, at least in sign, with our radial migration results. In order to dispel this confusion, we carefully verify our analytic predictions with numerical simulations in Sections 3 and 4 below.

We can make use of Eq. (9) to gain additional insight into the meaning of the three-body adiabatic invariant (Eq. 7). When A and μ are both very small, low inclination and eccentricity Trojan orbits, viewed in the frame which corotates with Jupiter, look like little ellipses centered on the Lagrangian equilibrium points with the ratios of their semimajor to semiminor axes equal to

$$\frac{a}{b} = \frac{2}{\sqrt{3\mu}} \qquad (12)$$

(Murray and Dermott 1999). The area within this ellipse is

$$\text{area} = \pi ab = \frac{\pi}{2}a^2\sqrt{3\mu}. \qquad (13)$$

For a small tadpole orbit, the libration amplitude times the semimajor axis of Jupiter's orbit is approximately equal to the major axis of the ellipse ($Aa_J \simeq 2a$). Thus we can rewrite Eq. (13) as

$$\text{area} = \frac{\sqrt{3}\pi}{8}\left(\frac{M_J}{M_S + M_J}\right)^{1/2} A^2 a_J^2 \qquad (14)$$

and then use Eq. (7) to eliminate A in favor of a_J:

$$\frac{\text{area}}{a_J^{3/2}} = \frac{J_{3\text{body}}}{3\sqrt{G(M_S + M_J)}} = \text{constant} \qquad (15)$$

The final equality holds for pure radial migration when M_S and M_J are both constant. For isotropic mass changes to either the Sun or Jupiter, we use Eq. (9) to eliminate the mass dependence and find

$$\frac{\text{area}}{a_J^2} = \text{constant} \tag{16}$$

Thus, during isotropic adiabatic mass accretion, the dimensionless area of small-amplitude Trojan orbits (i.e., the area enclosed by the orbit divided by the square of Jupiter's semimajor axis) is exactly preserved (Eq. 16). The response to direct radial migration induced by torques on Jupiter is only slightly different (Eq. 15). If Jupiter accreted its mass in an anisotropic way, a combination of the above two equations would apply. In the actual Solar System, the multiple doublings of the jovian mass predicted by the core-accretion model dominates the likely ~10% changes in a_J. Thus, to an excellent approximation, as Jupiter accretes mass, A decreases and the radial width of the Trojan orbit increases so that the area enclosed by the orbit remains constant (see Fig. 1). Note that the large libration amplitude of the tadpole in Fig. 1 violates one of our assumptions, and therefore departures from perfect area conservation are evident.

Finally, we can use Eq. (9) to determine what effect changing the mass of the Sun has on the libration amplitudes of Jupiter's Trojans. The dependence of A on M_S is present in Eq. (8) through the factor $(a_{Jf}/a_{Ji})^{-1/4}$. If the mass of the Sun is altered slowly and isotropically, Eq. (9) shows that a_J will change according to

$$\frac{a_{Jf}}{a_{Ji}} = \frac{M_{Si} + M_J}{M_{Sf} + M_J}. \tag{17}$$

Combining this with Eq. (8), we find

$$\frac{A_f}{A_i} = \left(\frac{a_{Jf}}{a_{Ji}}\right)^{-1/4} = \left(\frac{M_{Sf} + M_J}{M_{Si} + M_J}\right)^{1/4}. \tag{18}$$

Thus, slowly and isotropically adding mass to the Sun increases the libration amplitude of the Trojan, which is the opposite of the effect on A caused by adding mass to Jupiter.

2.2. Trojan Inclination and Eccentricity

Additional adiabatic invariant calculations determine the effects of changing Jupiter's mass and semimajor axis on a Trojan asteroid's eccentricity, e_a, and inclination, i_a. For the case when $i_a \neq 0$, we approximate the orbit of the Trojan as an inclined circle. Then, the motion of the asteroid in the z-direction can be well represented by simple harmonic motion with a restoring force equal to the sum of the z-components of the gravitational forces of the Sun and Jupiter acting on the asteroid. If we assume that the asteroid's inclination and libration amplitude are small, the distances between Jupiter, the asteroid, and the Sun are all approximately equal to a_J. Then, the restoring force per

unit mass acting on the asteroid is

$$f = \frac{-G(M_S + M_J)}{a_J^3} z, \tag{19}$$

where z is the distance of the Trojan asteroid above the plane of Jupiter's orbit. Notice that the vertical oscillation frequency is the same as Jupiter's orbital frequency (Eq. 3). The Hamiltonian for the vertical motion is

$$H = \frac{1}{2}\dot{z}^2 + \frac{1}{2}\frac{G(M_S + M_J)}{a_J^3} z^2, \tag{20}$$

which has canonical variables $q = z$ and $p = \dot{z}$. As in Section 2.1, for an adiabatic change to the system, the action is conserved. Noting that here adiabatic means that changes to the system are negligible over one orbital period, we find

$$J_{incl} = \int \dot{z}\, dz = \pi i_a^2 \sqrt{G(M_S + M_J)a_J} = \text{constant}, \tag{21}$$

where we have used the relation $z_{max} = a_J \sin i_a \simeq i_a a_J$ and integrated over a full orbital period. From this result, we see that if an external force adiabatically changes the semimajor axis of Jupiter's orbit about the Sun, the inclination of the Trojan will change according to the relation

$$\frac{i_{af}}{i_{ai}} = \left(\frac{a_{Jf}}{a_{Ji}}\right)^{-1/4}. \tag{22}$$

If instead the mass of Jupiter or the Sun is varied, Eq. (21) tells us that some combination of i_a and a_J must change to keep the action constant. For an isotropic mass loss or gain, we can use Eq. (9) to determine how the variation is shared between i_a and a_J. Combining Eq. (21) with Eq. (9), we find

$$i_a = \text{constant}, \tag{23}$$

which holds for changes in either M_J or M_S.

The adiabatic calculation for an eccentric asteroid orbit parallels that for an inclined orbit; however, the radial oscillation frequency is given by

$$n_{radial} = \left[\frac{G\left(M_S - \frac{27}{4}M_J\right)}{a_J^3}\right]^{1/2} \tag{24}$$

(Murray and Dermott 1999, p. 94) rather than by Eq. (3). Accordingly, the action, evaluated for small eccentricities, has the form

$$J_{ecc} = \int \dot{r}\, dr = \pi e_a^2 \sqrt{G\left(M_S - \frac{27}{4}M_J\right)a_J} = \text{constant}, \tag{25}$$

TABLE II
Reaction of Orbital Parameters to Imposed Adiabatic Changes in a_J, M_J, and M_S

	If a_J slowly decreased	If M_J slowly increased	If M_S slowly increased
Then a_J	X	Decreases (Eq. 10)	Decreases (Eq. 17)
Then A	Increases (Eq. 8)	Decreases (Eq. 11)	Increases (Eq. 18)
Then e_a	Increases (Eq. 26)	Slightly increases (Eq. 27)	Slightly decreases (Eq. 27)
Then i_a	Increases (Eq. 22)	Is unaffected (Eq. 23)	Is unaffected (Eq. 23)

and e_a will respond to an adiabatic change in a_J according to the relation

$$\frac{e_{af}}{e_{ai}} = \left(\frac{a_{Jf}}{a_{Ji}}\right)^{-1/4}. \tag{26}$$

This result agrees, at least in sign, with analytic work by Gomes (1997), who showed that e_a would increase when a_J was decreased. For variations in M_S and/or M_J, we combine Eqs. (9) and (25), and find that

$$e_a\left(1 - \frac{31}{16}\frac{M_J}{M_S}\right) = \text{constant}. \tag{27}$$

Thus, an isotropic increase in Jupiter's mass should lead to a slight increase in a Trojan asteroid's eccentricity.

In summary, for adiabatic changes to the Sun–Jupiter–Trojan system, we find that if the semimajor axis of Jupiter is decreased, the asteroid's libration amplitude (Eq. 8), eccentricity (Eq. 26), and inclination (Eq. 22) will all increase. Furthermore, if we increase Jupiter's mass isotropically, a_J will decrease (Eq. 10) and the Trojan's libration amplitude will decrease (Eq. 11), its eccentricity will increase slightly (Eq. 27), and its inclination will remain unchanged (Eq. 23). Finally, if the Sun's mass is increased isotropically, a_J will be decreased (Eq. 17) and the asteroid will be dragged inward with Jupiter, A will increase by the same amount it would were a_J altered by an external torque (Eq. 18), e_a will decrease slightly (Eq. 27), and i_a will not change (Eq. 23). These results are summarized in Table II.

3. NUMERICAL WORK: JUPITER'S MASS GROWTH BY ACCRETION

In this section and the next, we confirm the analytic results above and explore their range of validity by numerically integrating the three-body system consisting of the Sun, Jupiter, and a massless asteroid. The full equations of motion, consisting of the gravitational force of each body acting on the other two, are integrated in inertial coordinates. We use Bulrisch–Stoer and Runge–Kutta methods with adaptive stepsize (Press *et al.* 1987), having initially decided against faster symplectic methods (Wisdom and Holman 1991) because of the difficulty in handling close approaches with Jupiter. Although fast symplectic methods for handling close approaches do exist (Duncan *et al.* 1998), the speed of our routines was adequate. We ran extensive tests on our code, including checking that the Bulrisch–Stoer and Runge–Kutta integrators converged to the same solutions, producing plots which matched specific Trojan asteroid orbits illustrated in Murray and Dermott (1999, p. 97 and 98), and verifying that the Jacobi constant was conserved to sufficient accuracy for the circular restricted three-body problem with constant Jupiter mass and semimajor axis.

We begin our numerical exploration by integrating the three-body system as Jupiter grows from $\sim 10 M_\oplus$ to its current mass. We experimented with growing Jupiter both exponentially ($M_J = M_{Ji} e^{\alpha t}$) and linearly ($M_J = M_{Ji} + \beta t$), where M_{Ji} is the initial mass of Jupiter and α and β are constants. We found, as expected from Section 2, that our results were not significantly affected by the form of mass growth so long as the growth was slow enough to be adiabatic; accordingly all results presented below are for an exponentially growing Jupiter. Additionally, orbits librating around the Lagrangian equilibrium point L4 behaved similarly to orbits around L5, as suggested by our analytic analysis. Thus, the results presented below apply to objects librating about either of these points.

3.1. Circular Coplanar Orbits

3.1.1. Dependence on mass growth time scales. Placing the Sun, Jupiter, and the asteroid all on initially circular coplanar orbits, we carry out a set of integrations in which Jupiter grows on time scales ranging from 10^2 to 10^5 years. We monitor the changes to the asteroid's libration amplitude and plot our results in Fig. 2.

For long mass growth time scales ($\sim 10^4$ years), the numerical asteroid orbits agree well with the analytic prediction. Initially, the numerically determined points track the analytic prediction precisely, but as Jupiter's mass grows the points begin to scatter more. The increase in the amplitude of the oscillation of the numerical points about the analytically predicted line is due to limitations of our method of calculating the libration amplitude. We use an analytic approximation (Yoder 1983, Shoemaker *et al.* 1989) which makes the following assumptions: (1) a planar three-body system with all the objects on circular orbits, (2) $M_a \ll M_J \ll M_S$, and (3) A is very small. The Sun–Jupiter–Trojan system is reasonably approximated by these assumptions; however, as M_J/M_S grows, the error in the approximation increases, thereby causing an increased scatter of the calculated points. Furthermore, the changing mass of Jupiter itself leads to additional effects which are not accounted for in the simple theory; these effects are larger for more rapid growth time scales. Runs with slower growth time scales of $\sim 10^5$ years (not shown) exhibit the same behavior as the 10^4-year runs shown here, since both of these slow growth rates represent changes to the system that are well within the adiabatic limit where Eq. (8) is valid.

For the faster Jupiter growth rates (10^2 and 10^3 years), the numerical curves deviate substantially from the analytic prediction
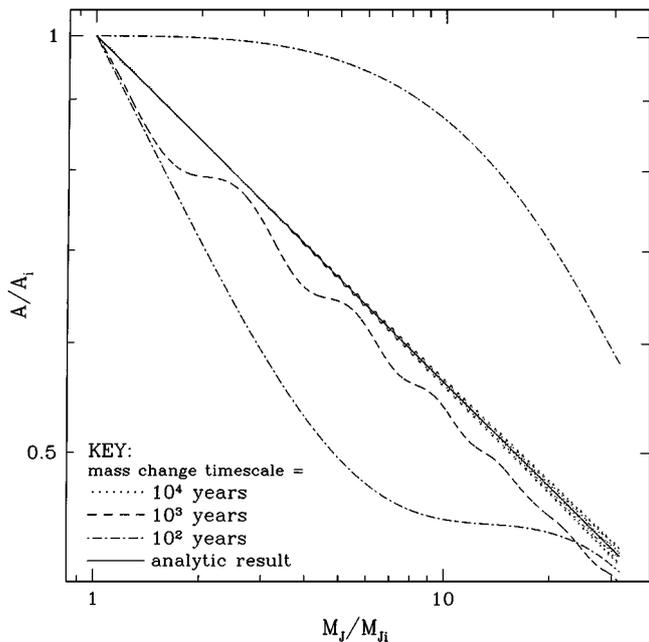
FIG. 2. The Trojan libration amplitude, A (normalized to its initial value, A_i) is plotted against Jupiter's mass, M_J (normalized to its initial value, M_{Ji}) on log–log scale for a series of integrations during which Jupiter grows from $\sim 10 M_\oplus$ to its current $\sim 320 M_\oplus$. The initial Trojan orbits are small ($A \simeq 10°$) tadpoles. The analytic prediction of Eq. (8) is plotted as a solid line. The numerical curve for the 10^4-year growth rate (dotted line) overlays the analytic result. Curves for longer growth time scales (not shown) agree equally well. The curves for shorter time scales, however, deviate significantly from the analytic curve in a manner which depends on the initial conditions of the orbit. Note that the two curves for the 10^2-year time scale differ only in the initial librational phase of the orbit.

of Eq. (8) (Fig. 2). In these cases, significant changes in the mass of Jupiter occur on time scales comparable to the libration period of the Trojan asteroid, $T = \frac{2\pi}{\omega}$ (with ω given by Eq. 5), which is ~ 900 years for $M_J = 10 M_\oplus$ and ~ 150 years for Jupiter's current mass. Thus, the change in the Trojan orbit depends on its initial conditions, i.e., exactly where along the tadpole orbit the asteroid starts. The initial conditions for the 10^3-year time scale run shown in Fig. 2 are chosen so that the curve exhibits maximum deviation from the analytic result. Note that the oscillations in this curve are not due to inaccuracies in the analytic approximation used to calculate the libration amplitude; they are real effects due the asteroid's librational motion and occur at the libration frequency. Unlike the artificial oscillations in the 10^4-year curve, the physical oscillations in the 10^3-year curve never cause A to increase.

The dependence of short time scale runs on initial conditions is clearly illustrated by the curves for two extreme choices of asteroid starting point for the 10^2-year time scale plotted in Fig. 2. The curve which is everywhere above the analytic line corresponds to an asteroid which was started at the point along the tadpole orbit farthest away from Jupiter (maximum ϕ, see Fig. 1). The basic characteristics of this curve can be understood using a simple harmonic oscillator analogy: we treat the librational

motion of the asteroid as a one-dimensional oscillation in the ϕ direction, and the rapid growth of Jupiter in 10^2 years is approximated as instantaneous growth. Using this analogy, growing Jupiter when the asteroid starts at the farthest point from Jupiter is equivalent to increasing the restoring force of the harmonic oscillator instantly when the oscillator is at its maximum extension. This affects the period of the oscillations, but leaves the amplitude unchanged. For this reason, the upper 10^2-year curve in Fig. 2 is initially horizontal, indicating no change in the libration amplitude. Since increasing Jupiter's mass over 10^2 years is not truly an instantaneous change, the libration amplitude of the Trojan asteroid eventually decreases as it begins to move toward Jupiter.

The 10^2-year time scale curve in Fig. 2 which is everywhere below the analytic line corresponds to an asteroid started at the point on the tadpole orbit farthest from the Sun (see Fig. 1) where $|\dot{\phi}|$ is maximum. Again using the harmonic oscillator analogy, this is equivalent to increasing the restoring force when the oscillator has its maximum velocity. This causes the amplitude of the oscillations to decrease. Thus, we see an initially rapid decrease in the Trojan's libration amplitude which slows as the asteroid moves closer to Jupiter.

In the adiabatic limit, the effect of the mass change is averaged over all points along the asteroid's orbit. Thus, the decrease in the asteroid's libration amplitude for adiabatic growth lies between the two extremes just discussed, as can be seen in Fig. 2.

3.1.2. Dependence on libration amplitude. Next, we explore the role of the asteroid's initial libration size in determining how its libration amplitude will change as Jupiter's mass grows. Recall that the analytic prediction (Eq. 8) was derived with the assumption of small libration amplitude. We study a set of tadpoles with different initial libration amplitudes; in each integration the time scale for Jupiter's mass growth is 10^5 years, well within the adiabatic limit. We find that for initial libration amplitudes $\lesssim 50°$, our numerical results agree well with the analytic prediction, as expected (Fig. 3). The curve for the $A_i \simeq 50°$ tadpole shows a slight deviation from the analytic result; tadpoles with larger initial amplitudes show even greater departures. As in Fig. 2, the spread of the numerical points is due to the analytic method used to determine the libration amplitude.

The larger tadpole orbits shrink more rapidly than Eq. (8) predicts. Furthermore, the larger the libration amplitude is, the faster it shrinks, as can be seen by examining the initial slopes of the curves for the $110°$, $130°$, and $150°$ tadpoles in Fig. 3. This can be understood by considering the effective potential in the corotating reference frame (Fig. 1). The effective potential changes much more steeply at the head of the tadpole near Jupiter than at the tail which lies further away (Erdi 1997). The larger the tadpole orbit is, the further it extends away from Jupiter, and the less steep is the potential in which the tail end of the orbit lies. When the potential is flatter, the location of the turning point of the orbit changes by a greater amount for the same change in energy, and so the orbits whose tails lie in the shallowest potential, i.e., those with the largest libration amplitude, shrink the fastest
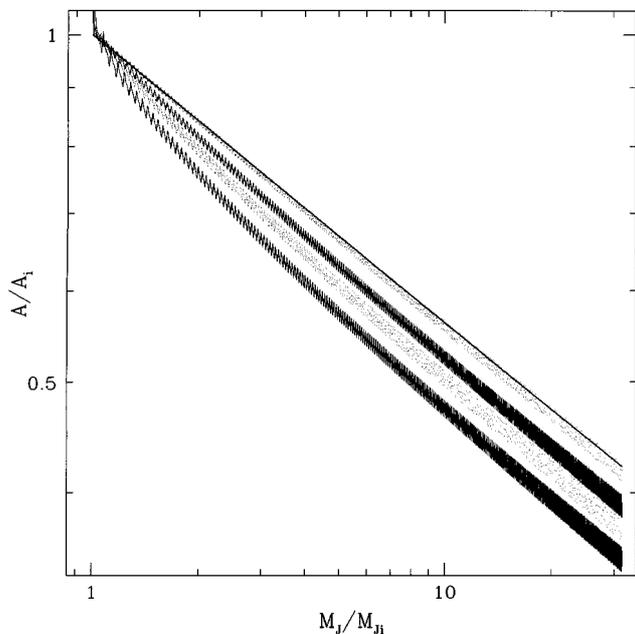
FIG. 3. The Trojan libration amplitude (normalized to its initial value) is plotted on a log–log scale for a variety of different-sized initial tadpole orbits as Jupiter grows from $\sim 10 M_\oplus$ to its present mass. Our analytic result (Eq. 8) is plotted as a heavy solid line. The upper dotted curve, which overlays the theoretical line, is for a tadpole with $A \simeq 50°$ initially. All smaller tadpoles (not shown) agree even better with the analytic prediction. The lower curves in this figure are tadpoles with (from top to bottom) $110°$, $130°$, and $150°$ initial libration amplitudes. The large tadpole orbits shrink faster than our analytic work predicts. The oscillations in the numerical curves are a result of the analytic approximation used to calculate the libration amplitude and occur at the libration frequency.

(see Fig. 4). Once the initially large tadpole orbits become small enough, they shrink at the rate predicted by Eq. (8). This is illustrated in Fig. 3 where, by the end of the integrations, all of the curves are tending to the same slope as the analytic result.

3.1.3. Horseshoe orbits. We also examine the effects of Jupiter's mass growth on very large "horseshoe orbits" whose librations encompass both the L4 and L5 equilibrium points. Figure 4 shows the results of an integration in which the asteroid has an initial libration amplitude of $\sim 330°$. The horseshoe orbit shrinks slowly until $\sim 1.3 \times 10^4$ years when it transitions to an L4 tadpole. The tadpole then continues to shrink.

Although horseshoe orbits are well outside the range of libration amplitudes described by our adiabatic calculation, they too shrink under the influence of a growing Jupiter. The rate of decrease in libration amplitude is, however, different for horseshoe orbits and tadpole orbits. Looking at the lower edge of the plot in Fig. 4, we see that the turning point of the horseshoe orbit pulls away from Jupiter at a nearly constant rate for exponential growth of Jupiter's mass. Furthermore, the corresponding turning point in the tadpole orbit (the tip which lies nearest Jupiter) pulls away approximately linearly as well, but with a shallower slope. For a doubling of Jupiter's mass, one tip of the horseshoe orbit recedes from Jupiter by $\sim 4.5°$, while for the same mass

change, the near-Jupiter tip of the tadpole moves by only $\sim 3.0°$. In this way, horseshoe orbits shrink even faster than tadpole orbits.

Further integrations demonstrate that the growth of Jupiter to its current mass captures most asteroids which were initially on horseshoe orbits into tadpole orbits. Figure 5 shows the results of a set of integrations which determine the fate of asteroids placed into different-sized horseshoe orbits at various points during the growth of Jupiter. We find that if the asteroids are placed on horseshoes when Jupiter is a $10 M_\oplus$ core, orbits with initial libration amplitudes as large as $A \sim 346°$ are captured into tadpole orbits by the time Jupiter has reached its present mass. When the asteroids are started on horseshoes after Jupiter has already grown partway to its current mass, fewer of the orbits shrink sufficiently to transition to tadpoles; however, even if the asteroids are started when Jupiter has reached three-quarters of its final mass, some of the smaller horseshoe orbits still become tadpoles, at least temporarily, during the course of the integration.

In Fig. 5, we can clearly see the chaotic nature of the evolution of the horseshoe orbits: there is mixing between the orbits which
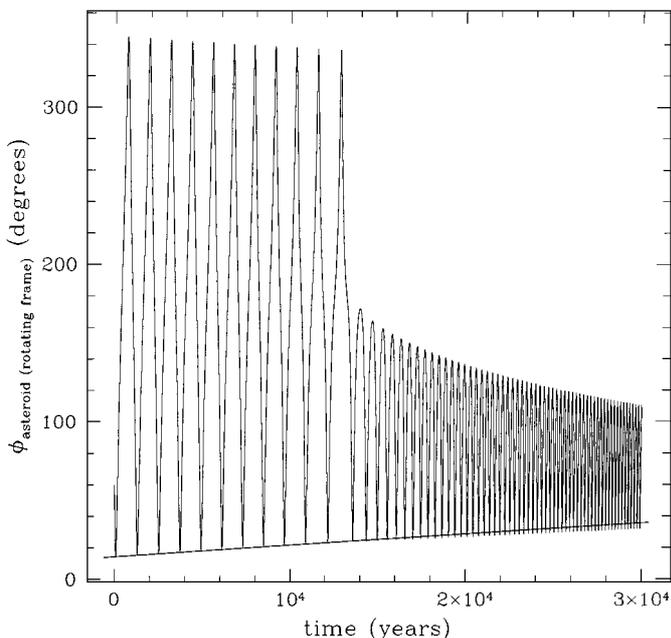

FIG. 4. Here we show the behavior of ϕ, the longitude of the asteroid in the frame which corotates with Jupiter, as Jupiter grows from $\sim 10 M_\oplus$ to its present mass in 3×10^4 years. Jupiter is at $\phi = 0°$, and the initial asteroid orbit is an $A \sim 330°$ horseshoe. At $\sim 1.3 \times 10^4$ years the orbit jumps to an L4 tadpole with $0° \leq \phi \leq 180°$. The Trojan's libration period is initially about ~ 1200 years and decreases to ~ 600 years when the horseshoe transfers to a tadpole. Afterward, the tadpole's libration period continuously shortens in accordance with Eq. (5). Note that the tadpole orbit shrinks most rapidly when its tail (i.e., its away-from-Jupiter turning point) is near $\phi = 180°$, since the effective potential is flattest there. Further, observe that the lower edge of the plot has a steeper slope for the horseshoe orbit than for the tadpole orbit; the straight line overlaying the plot is fit by eye to the edge of the horseshoe orbit and has a slope of $\sim 4.5°$ per Jupiter mass doubling.
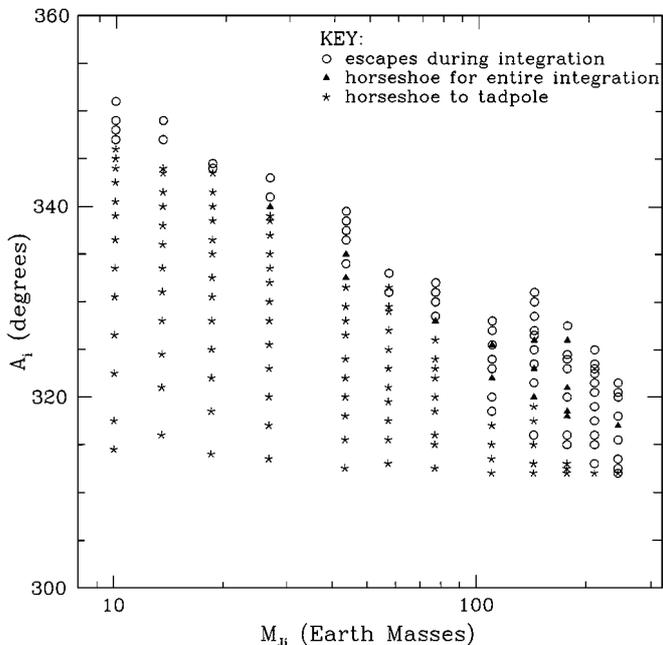
FIG. 5. This plot shows the final state of asteroids started on $e = 0$ horseshoe orbits at different points during Jupiter's growth to its current size of $320 M_\oplus$. The vertical axis shows the initial libration amplitude of the horseshoe orbit and the horizontal axis shows the mass of Jupiter when the asteroid was placed in that orbit. Asteroids which escaped from the 1:1 resonance during the 10^5 years of the integration are indicated by open circles. Objects which remained in horseshoe orbits for the entire integration are shown as filled triangles, and asteroids which were captured into tadpole orbits are shown as stars. Most, but not all, of the orbits which became tadpoles remained tadpoles for the rest of the integration. The mixing of final states seen here is an indication of the chaotic nature of the orbits.

escape the system and those which remain in horseshoes for the entire time. We also observe mixing at the boundary for capture into tadpoles. Small differences in the initial asteroid orbits can significantly alter the effects of jovian perturbations, vastly changing the final asteroid orbit. Additionally, note that the smallest possible horseshoe orbits occur at $A \sim 312°$, nearly independent of the mass of Jupiter. This result is in agreement with the analytic work of Horedt (1984) and Morais (1999). The transition to a tadpole orbit occurs whenever a horseshoe orbit shrinks to this minimum size.

Data from the integrations plotted in Fig. 5 confirm that the observation made from Fig. 4, that each tip of a horseshoe orbit recedes from Jupiter at a roughly uniform rate of $\sim 4.5°$ per Jupiter doubling, holds for general horseshoe orbits. Figure 6 shows the decrease in the libration amplitudes of the horseshoe orbits plotted against the number of doublings of Jupiter's mass. The solid line, fit by eye to the data, has a slope of $9.0°$ per doubling (indicating that each of the two orbital turning points recedes at half that rate). The slight flattening of the data points near (0, 0) on the plot indicates that the horseshoe orbits shrink a bit more slowly when they are near the transition to tadpole orbits. We verified this observation with additional simulations not shown here. In order to get the best value for the slope in

Fig. 6, we ignored the points in the flattened tail of the plot and did not insist that our fitted line go through (0, 0).

Next, we look at the final sizes of the tadpoles produced by the transitions from horseshoes shown in Fig. 5 to see if these objects could, in fact, contribute to the current population of Jupiter Trojans. In Fig. 7, we see that a small number of the asteroids placed in horseshoe orbits when Jupiter is $\lesssim 10\%$ of its final mass become tadpole orbits which are stable for a significant fraction of the age of the Solar System. A substantially larger number of the horseshoe orbits started when Jupiter is $\lesssim 20\%$ of its final mass become tadpoles that remain stable for at least a hundred million years. Thus, assuming that objects resided on horseshoe orbits when Jupiter was accreting mass, a small fraction of these objects may still survive in the Trojan swarm today. Furthermore, since these asteroids undergo relatively frequent collisions (Marzari *et al.* 1997), they almost certainly produced some fragments which were ejected into more stable tadpole orbits.

3.2. Eccentric and Inclined Trojan Orbits

To further explore the range of validity of our analytic results from Section 2 above, we add eccentricity and inclination to the Trojan orbit, at first leaving Jupiter on a circular orbit. We integrate the three-body system for a number of different small values of eccentricity and inclination ($e_a \lesssim 0.1$, $i_a \lesssim 1°$) with the Trojan on a small ($A \sim 10°$) tadpole orbit and Jupiter growing over 10^5 years. We find that for these low values of eccentricity
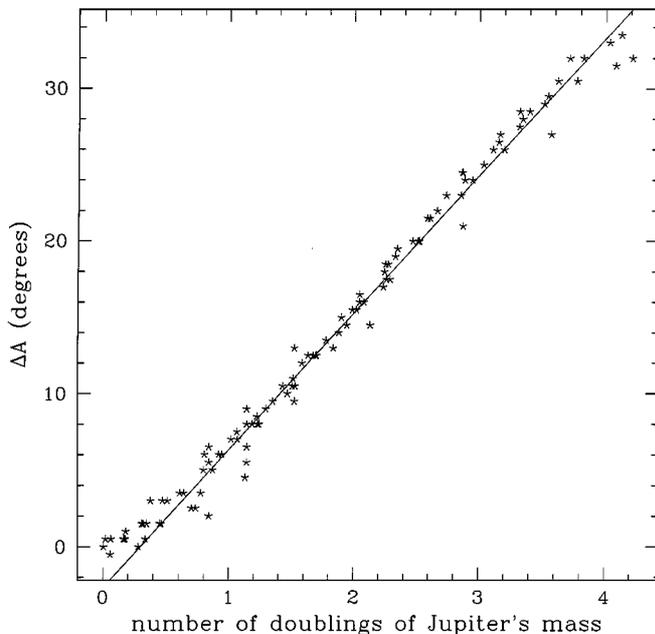

FIG. 6. This plot shows the decrease in the libration amplitudes of those horseshoe orbits from Fig. 5 which did not escape the 1:1 resonance plotted against the number of secondary mass doublings. A line with a slope of $9.0°$ per doubling was fitted by eye to the data. The low scatter of the points about this line indicates that the decrease in A by $9.0°$ per doubling is a general property of horseshoe orbits, independent of the mass of the secondary.
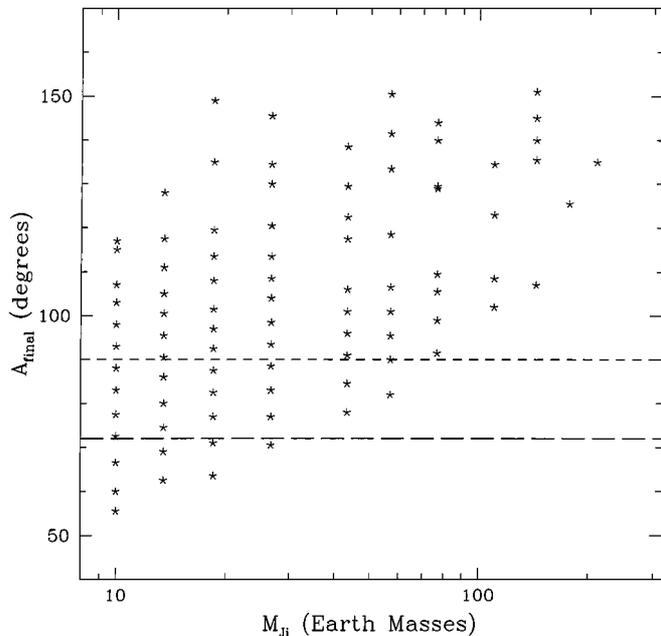
FIG. 7. This plot shows the final libration amplitudes of the asteroids from Fig. 5 which were on tadpole orbits at the end of the 10^5-year integration. The horizontal axis is the mass of Jupiter at the time when the asteroids were placed into their initial horseshoe orbits. The orbits represented by points below the long-dashed line are stable for more than 10^9 years, while those below the short-dashed line are stable for greater than 10^8 years. These time scales are estimated from the work of Levison *et al.* (1997) for tadpoles with zero eccentricity.

FIG. 8. The square data points show our numerical measurements of the change in the libration amplitude of a Trojan asteroid with $A_i \simeq 10°$, $e_a \simeq 0.01$, and $i_a \simeq 1°$ as Jupiter (on a circular orbit) grows from $\sim 10 M_\oplus$ to its current mass in 10^5 years. Representative error bars are shown for two data points. The solid line is the analytic prediction for $e_a = i_a = 0$ (Eq. 8). The numerical points agree with the analytic curve to within the error bars.

and the inclination, our analytic expression for the change in libration amplitude (Eq. 8) still approximates the behavior of the system well. Figure 8 shows the results of one of our numerical integrations. The asteroid is given an initial eccentricity of $e_a \sim 0.01$ and an initial inclination of $i_a \sim 1°$. The analytic method of Yoder *et al.* (1983) for determining the libration amplitude, A, fails for nonzero e_a and i_a, so we resort to a simpler but more time-consuming method. The values of libration amplitude are determined from the numerical data by taking the average of the local maximum and minimum values of ϕ at the turning points ($\dot{\phi} = 0$) of the tadpole orbit. The range in values of ϕ at the turning points is due to both the eccentricity and the inclination of the orbit. The averaging process takes advantage of the difference in orbital and librational time scales and is essentially the guiding center approximation for the orbit (Murray and Dermott 1999). The remaining uncertainty in the numerical points is due primarily to the difficulty in determining the maximum and minimum ϕ values from a sample of discrete points. Further, as the libration period becomes smaller, we sample only parts of the elliptical orbit during the turning point. Despite these difficulties, we find that the numerical points in Fig. 8 follow the analytic curve well.

We also explore the effects of Jupiter's mass growth on the eccentricity and inclination of Trojan orbits. Figure 9 shows the eccentricity and inclination of the Trojan orbit whose libration amplitude is plotted in Fig. 8. We see that, to first order, the
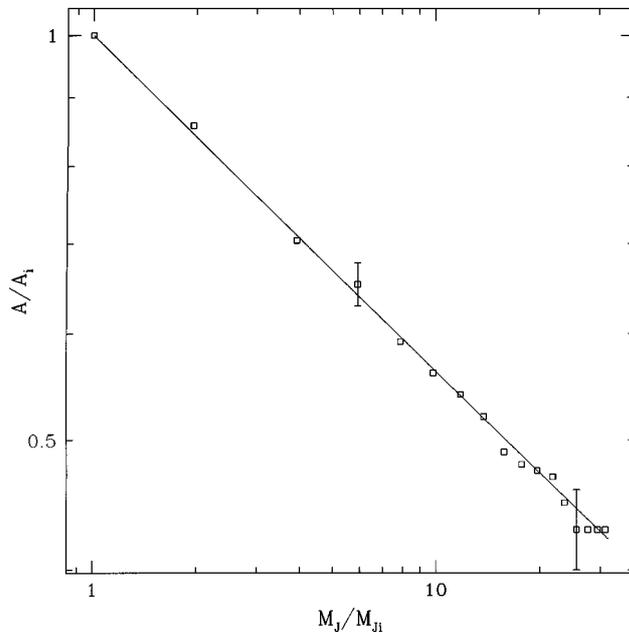
eccentricity and inclination are constant during Jupiter's growth, as predicted in Section 2.2. A closer inspection reveals a slight increase in the mean eccentricity which is in good agreement with the analytical predictions of Eq. (27).
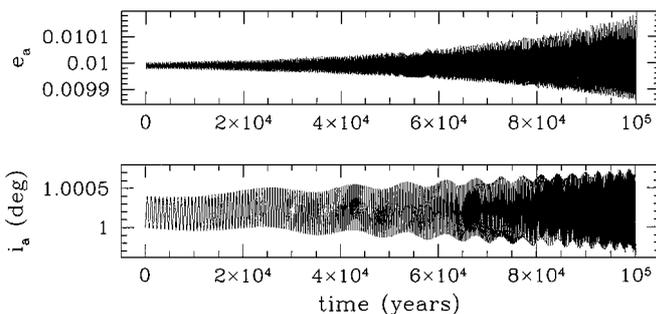

FIG. 9. This plot shows the eccentricity and inclination of the tadpole orbit whose libration amplitude is plotted in Fig. 8. The mean values of the asteroid's eccentricity and inclination are essentially unchanged (note the vertical scale) by the growth of Jupiter's mass, although the tiny increase in the mean eccentricity is real. The mean eccentricity rises by approximately one small tick mark over 10^5 years, which is consistent with the $\sim 0.2\%$ increase predicted by Eq. (27). The high-frequency oscillations visible in the traces of both e_a and i_a are due to the Trojan's librational motion and thus become more rapid as Jupiter's mass increases, in accordance with Eq. (5). The low-frequency oscillations in the inclination are correlated to the precession of the asteroid's pericenter (not shown) driven by the disturbing effects of Jupiter. Since all the oscillations are caused by jovian perturbations, they increase in amplitude as Jupiter's mass grows.
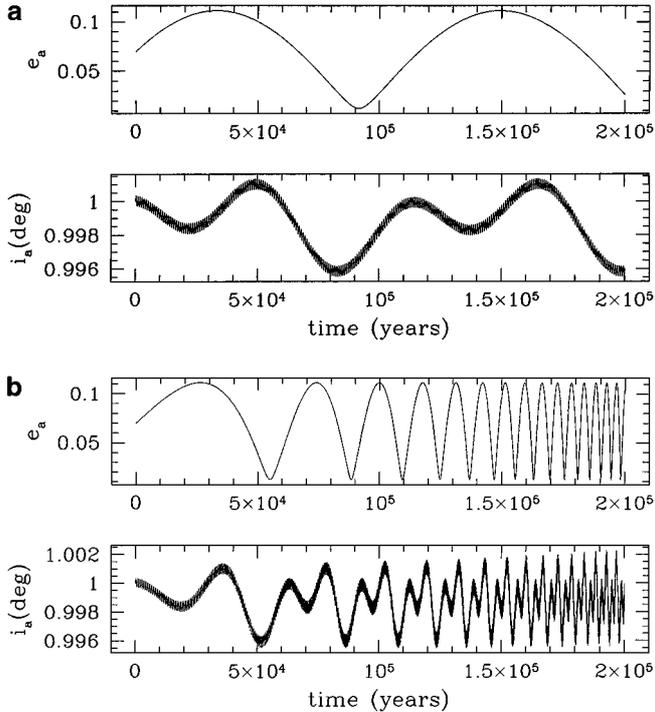
FIG. 10. These plots compare the orbital evolution of a Trojan asteroid (a) without and (b) with jovian mass growth. For both cases, the Trojan asteroids start with identical initial conditions and Jupiter has an eccentricity of 0.05. In (a), the mass of Jupiter is kept constant at $\sim 10 M_{\oplus}$, while in (b) Jupiter's mass grows from $\sim 10 M_{\oplus}$ to its current mass in 2×10^5 years. Both e_a plots show oscillations about a forced eccentricity equal to Jupiter's eccentricity. The plots of i_a show the free inclination (since $i_{(forced)a} = 0$). The high-frequency oscillations in i_a are caused by the Trojan's librational motion, while the low-frequency ones are correlated to the oscillations in e_a. The free and forced eccentricities and inclinations of the Trojan asteroid are essentially unchanged by Jupiter's growth, as predicted in Section 2.2; however, the frequencies of all the observed oscillations in e_a and i_a increase as Jupiter's mass grows.

3.3. Eccentric Jupiter Orbit

Finally, we add eccentricity to Jupiter's orbit while keeping the Trojan on an inclined and eccentric orbit. Figure 10a shows the eccentricity and inclination of a Trojan when Jupiter has a constant mass and an eccentricity, $e_J = 0.05$. The asteroid's eccentricity oscillates around a constant "forced" component which is equal to the eccentricity of Jupiter. The "free" component of the eccentricity is approximately the amplitude of the oscillations (~ 0.05 in Fig. 10a). The Trojan's forced inclination is zero, since the inclination is measured relative to Jupiter's orbit. The high-frequency oscillations visible in the plot of i_a are due primarily to the Trojan's librations, while the lower frequency oscillations in i_a are correlated to the oscillations of the Trojan's eccentricity.

Starting with the same initial orbits for both Jupiter and the Trojan, but allowing Jupiter to accrete material over 2×10^5 years, we obtain the results shown in Fig. 10b. The values of the forced and free eccentricities and inclinations are not significantly altered by Jupiter's growth; however, the frequen-

cies of the oscillations in both e_a and i_a increase as the mass of Jupiter grows, and the strength of its gravitational perturbation increases. The slight upward drift in the mean Trojan inclination seen in Fig. 10b is simply part of a periodic oscillation in i_a correlated to the drift of the orbital node. So, as predicted in Section 2.2, we find that the eccentricity and inclination of a Trojan orbit remain essentially unchanged as Jupiter's mass grows, even when Jupiter is on an eccentric orbit. Thus, the primordial eccentricities and inclinations of some large Trojan objects may have been preserved during Jupiter's accretion of mass.

4. NUMERICAL WORK: RADIAL MIGRATION OF JUPITER

We now turn to a series of integrations of the three-body Sun–Jupiter–asteroid system in which Jupiter undergoes 1 AU of inward radial migration. For our integrations, we set Jupiter's initial semimajor axis to ~ 6.2 AU and leave its mass constant at $\sim 10 M_{\oplus}$. Because the effects of Jupiter's radial migration are independent of Jupiter's mass and depend only on the ratio of the initial and final semimajor axes (see Eqs. 8, 22, and 26), our numerical results are applicable to migration of Jupiter at any point during its history.

The amount of radial migration that Jupiter underwent as a rocky core and growing gas giant due to tidal interactions with the gas and planetesimal disks is poorly constrained, but might be several AU (Ward 1997). Furthermore, after attaining its present mass, Jupiter continued to experience radial migration due to scattering of planetesimals by the giant planets (dynamical friction); recent models for the formation of the Oort Cloud (Fernandez and Ip 1996, Hahn and Malhotra 1999) predict several tenths of an AU of radial migration at this stage. Our results may be scaled to either or both of these scenarios.

We artificially cause Jupiter's orbit to shrink by applying a drag force of the form $\mathbf{F} = -k\mathbf{v}_J$ (where $\mathbf{v}_J$ is Jupiter's heliocentric velocity and k is the drag constant) which acts only on Jupiter. This form of drag affects Jupiter's semimajor axis, but not its eccentricity, providing a "simplest case" for studying the effects of Jupiter's radial migration on Trojan objects. Recall that our analytic work shows that, in the adiabatic limit, changes in the Trojans' libration amplitudes are independent of the exact form of the drag force (see Eq. 8); thus our choice for the form of the drag force is reasonable. As in the integrations for Jupiter's mass growth, we find no apparent dependence on the choice of Lagrangian equilibrium point, so the results below are equally applicable to orbits about the L4 and L5 points.

4.1. Circular Coplanar Orbits

4.1.1. Dependence on radial migration time scale. We initially place the Sun, Jupiter, and the asteroid all on circular coplanar orbits. We carry out a set of integrations with the Trojan on a small tadpole orbit using different drag coefficients, k, to cause Jupiter to migrate inward by ~ 1 AU on time scales ranging from $\sim 10^2$ to $\sim 10^5$ years. For slow evolution, we observe that the Trojans are always dragged inward with Jupiter. As in the

case of Jupiter's mass growth (Section 3.1.1), we find that for time scales significantly larger than the Trojan libration period (~1000 years for $M_J = 10M_\oplus$ and $a_J = 6.2$ AU), the libration amplitude of the Trojan increases in the manner predicted by Eq. (8). Also, as in the mass accretion case, when the migration time scale approaches the libration period, the change in libration amplitude deviates from our analytic prediction, with the direction and amount of deviation depending on the asteroid's initial librational phase.

For very fast migration rates, we find that the asteroid is not pulled inward with Jupiter, but instead is ejected from its tadpole orbit. For migration of Jupiter by ~1 AU in 10^3 years, one sample integration shows an initially small tadpole orbit transforming into a horseshoe orbit near the end of the integration. In another example, we change Jupiter's semimajor axis by an AU in 500 years and find that the asteroid escapes entirely from the 1:1 resonance after only ~300 years.

4.1.2. Dependence on libration amplitude. Next, we do a set of integrations starting the Trojan asteroid on different-sized tadpole orbits. In each run, we cause Jupiter to move from ~6.2 to ~5.2 AU over 10^5 years so that its migration is adiabatic. The results of several of these integrations are shown in Fig. 11. It is difficult to produce a plot similar to Fig. 3 because Yoder's (1979) formula for calculating the libration amplitude assumes
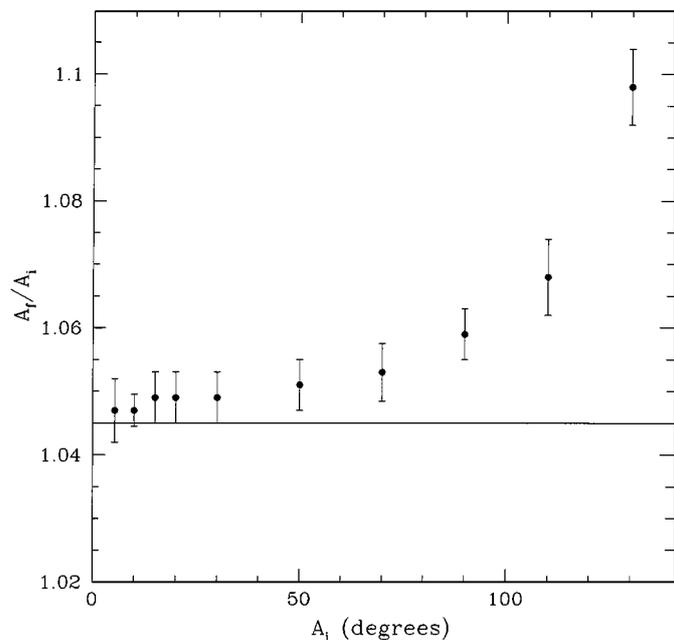
that there are no drag forces. Thus, we estimate the initial and final libration amplitudes by measuring the difference between the minimum and maximum values of ϕ for the first and last complete librations in the integration. Note that the torque on Jupiter causes the Trojans to librate about shifted equilibrium points; drag on a Trojan produces a similar shift (Murray 1994). In Fig. 11 we see that for small tadpoles ($A_i \lesssim 30°$) the numerical results agree well with the prediction of Eq. (8). The steplike appearance of the first five points reflects difficulties inherent in our measurement technique. As the initial libration amplitude becomes larger, however, the numerical points deviate increasingly from the analytic result. This is expected since the larger tadpoles break the assumption of small libration amplitude which was made during the derivation of Eq. (8). As in the case of Jupiter's mass growth, we see that for larger initial tadpoles, the change in libration amplitude is greater in magnitude but in the same direction as is predicted analytically. Also, we see that the deviation of A_f/A_i from the analytic prediction increases more steeply as the initial orbits become even larger. As was discussed in Section 3.1.2, this is caused by the shallow slope of the effective potential near the tail end (the end farthest from Jupiter) of large tadpole orbits.

4.2. Eccentric and Inclined Trojan Orbits

Next, we add eccentricity and inclination to the asteroid orbit, leaving Jupiter on a circular orbit. As in the case of Jupiter's mass growth, we find that small Trojan eccentricities and inclinations ($e \lesssim 0.1$, $i \lesssim 1°$) do not cause the behavior of the libration amplitude to deviate significantly from the analytic prediction of Eq. (8). However, unlike the mass growth case, Jupiter's migration does affect the eccentricity and inclination of the Trojan. Figure 12 shows the semimajor axis, eccentricity, and
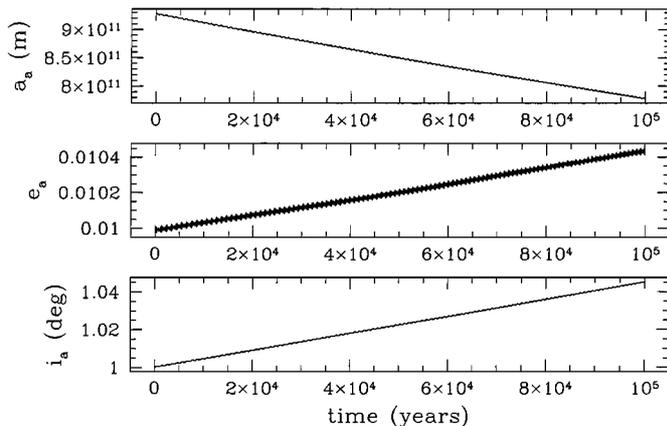
FIG. 11. This plot shows the ratio of final to initial libration amplitude for several different-sized tadpole orbits affected by the migration of Jupiter from ~6.2 to ~5.2 AU over 10^5 years. Jupiter is on a circular orbit. The results of numerical integrations are shown as solid dots with error bars which reflect the difficulties in measuring the libration amplitude. The horizontal line at $A_f/A_i = 1.045$ represents the analytic prediction of Eq. (8) which is valid only for small initial libration amplitudes. The numerical results agree well with the analytic prediction for $A_i \lesssim 30°$, but deviate increasingly from the prediction for larger initial libration amplitudes.

FIG. 12. This plot shows the change in the semimajor axis, eccentricity, and inclination of a Trojan asteroid on a slightly eccentric and inclined orbit as Jupiter (on a circular orbit) migrates radially from ~6.2 to ~5.2 AU in 10^5 years. The Trojan's eccentricity and inclination increase by a factor of $(a_{Jf}/a_{Ji})^{-1/4} = (6.2/5.2)^{-1/4} = 1.045$ as is predicted by Eqs. (22) and (26). Note that the tiny oscillations in e_a and i_a are due primarily to the Trojan's librational motion.

inclination of a Trojan asteroid on a small tadpole orbit as Jupiter migrates from ~6.2 to ~5.2 AU in 10^5 years. During that time, the asteroid's inclination increases from $1.000°$ to $1.045°$ and its eccentricity grows from 0.00999 to 0.01043, giving us $i_{af}/i_{ai} = 1.045 \pm 0.001$ and $e_{af}/e_{ai} = 1.044 \pm 0.001$. These agree well with the analytic prediction that $i_{af}/i_{ai} = e_{af}/e_{ai} = 1.045$, which we calculate using Eqs. (22) and (26). These changes in the asteroid's eccentricity and inclination resulting from ~1 AU migration of Jupiter are quite small, but are systematic.

4.3. Eccentric Jupiter Orbit

Finally, we explore the most general case of nonzero jovian eccentricity and a Trojan on an eccentric and inclined orbit. Figure 13 shows the semimajor axis, eccentricity, and inclination of a sample Trojan asteroid as Jupiter, with $e_J \sim 0.05$, migrates from ~6.2 to ~2.6 AU in 3×10^5 years. Note that we allow Jupiter to move by a much greater amount than in our earlier simulations so that the effects of migration can be more easily observed and quantified. As in Section 3.3, the asteroid has a forced eccentricity equal to Jupiter's eccentricity and a forced inclination of zero. The asteroid in Fig. 13 also has a free component of its eccentricity which is initially $\simeq 0.004$ and a free inclination which is initially $\simeq 1°$.

As Jupiter migrates inward, the free components of both the asteroid's eccentricity and its inclination increase systematically. From Fig. 13, we find $i_{(\text{free})af}/i_{(\text{free})ai} = 1.243 \pm 0.001$ and $e_{(\text{free})af}/e_{(\text{free})ai} = 1.32 \pm 0.15$. Both of these results agree well with the analytic prediction that $i_{af}/i_{ai} = e_{af}/e_{ai} = 1.243$ (Eqs. 22 and 26) for an adiabatic change in Jupiter's semimajor axis from 6.2 to 2.6 AU. Thus, our analytic results (Eqs. 22 and 26) hold even when Jupiter has a low eccentricity if e_a and i_a are interpreted as the free components of the asteroid's eccentricity and inclination.
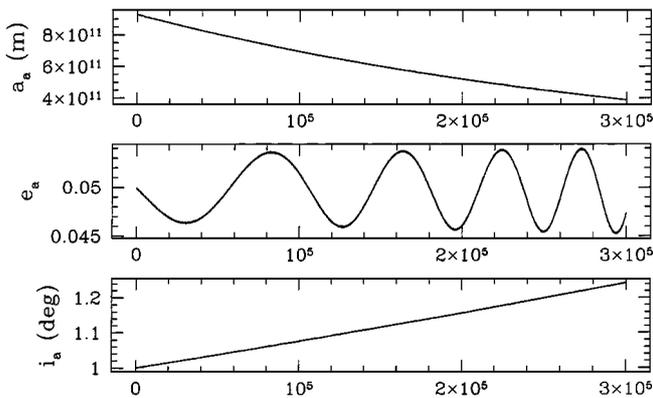

FIG. 13. This plot shows the semimajor axis, eccentricity, and inclination of a Trojan asteroid on a slightly eccentric and inclined orbit when Jupiter has an eccentricity of ~0.05 and migrates radially from ~6.2 to ~2.6 AU in 3×10^5 years. The forced components of both the asteroid's eccentricity and its inclination remain constant ($e_{(\text{forced})a} \sim 0.05$ and $i_{(\text{forced})a} = 0$); however, the free components of both e_a and i_a increase like $(a_{Jf}/a_{Ji})^{-1/4}$, as predicted by Eqs. (22) and (26).

5. DISCUSSION

We have shown with both a simple adiabatic calculation and numerical simulations that slow changes to the mass and semimajor axis of Jupiter cause the Trojan libration amplitude to vary according to the relation

$$\frac{A_f}{A_i} = \left(\frac{M_{Jf}}{M_{Ji}}\right)^{-1/4} \left(\frac{a_{Jf}}{a_{Ji}}\right)^{-1/4}$$

for Trojans with small libration amplitudes, small eccentricities, and small inclinations and Jupiter with a small eccentricity. For inclined and eccentric Trojan objects, we find that Jupiter's mass growth does not significantly affect either the Trojan's eccentricity or its inclination; however, Jupiter's radial migration causes a change in the free component of both of these quantities by a factor of $(\frac{a_{Jf}}{a_{Ji}})^{-1/4}$.

Applying our results to the core accretion model for the early evolution of Jupiter, we find that the planet's growth by gas accretion from a $\sim 10 M_\oplus$ core to its present mass would cause a decrease in the libration amplitude of any Trojan companions on small tadpole orbits to ~40% of their original size. Our representative choice for Jupiter's radial migration from ~6.2 to ~5.2 AU would result in an increase in the Trojans' libration amplitudes, eccentricities, and inclinations of only ~4%. Even for radial migrations of several tens of AU, the effects of Jupiter's mass growth dominate over the effects of its migration. Thus, the combined result of mass accretion and radial migration is to stabilize Trojan objects by systematically driving them to lower libration amplitudes. Also, our numerical integrations show that the libration amplitudes of Trojans on larger orbits shrink at an even faster rate. Further, the shrinking of horseshoe orbits due to Jupiter's growth could place additional objects or perhaps fragments of objects onto stable tadpole orbits. Thus, Jupiter's growth by mass accretion most likely played a significant role in the capture and evolution of the Trojan asteroid population.

Our results for the evolution of Trojan libration amplitudes, eccentricities, and inclinations are quite general and can be applied to other objects within the Solar System. For example, Eqs. (8), (22), and (26) predict that A, e, and i will all decrease substantially if the secondary body undergoes significant outward radial migration. Uranus and Neptune probably underwent more substantial radial migration due to dynamical friction with planetesimals than Jupiter, moving outward by as much as several AU (Fernandez and Ip 1996, Hahn and Malhotra 1999). This would have caused a decrease in A, e_a, and i_a of possible Trojan-like companions by about 10%. Radial migration effects might be even more significant for some planetary satellites, notably our Moon. The Moon is believed to have formed via a giant collision which produced a temporary ring of debris around the Earth (Canup and Esposito 1995, Ida *et al.* 1997). Such a process would have most likely captured some debris in librating orbits about the Moon's Lagrangian equilibrium

points. Over the subsequent 4.5×10^9 years, the Moon migrated outward to about 30 times its initial orbital radius. Ignoring other effects, this migration should have decreased the libration amplitudes, eccentricities, and inclinations of the debris particles to ~40% of their original values, stabilizing these objects in 1:1 resonance with the Moon. Since we observe no such objects today, either the 1:1 resonance was never populated or other effects (such as solar gravity) caused them to be unstable.

Another potential area for study is the satellite system of Saturn. The many resonances in this system are believed to have formed during the significant outward migration of these satellites due to both tidal interactions with Saturn and ring torques. One unexplained characteristic of the current Saturnian system is that, of the six largest satellites near Saturn, the middle two, Tethys and Dione, have a total of three Trojan companions but the others, Mimas, Enceladus, Rhea, and Titan, have none. This is curious because there is no obvious reason why the middle satellites should be the best at capturing Trojan companions. Also, the results of this paper suggest that the objects which migrate outward by the greatest amount should be the best at capturing and stabilizing their Trojan companions. This suggests that the inner two satellites, which have migrated farthest, should be most likely to have Trojan companions. It is likely that the probability of Trojan capture and the stabilization of Trojan orbits is complicated by the presence of resonances between the satellites. The inner four Saturnian satellites are all currently locked in resonances with each other, and they may have passed through various other resonances in the past. An exploration of the interactions between the migration process explored in this paper, and the effects of other resonances, discussed by Morais (2000), may provide insight into this unexplained characteristic of the Saturnian system. It may also provide insight into how the unusual pair of coorbital satellites, Janus and Epimetheus, which librate on horseshoe orbits, was formed in the Saturnian system.

Our work is also directly relevant to the capture of planetary satellites during the growth of the giant planets, as was suggested by Heppenheimer and Porco (1977). Equation (9) clearly shows that distant satellites would be drawn inward as a planet grows. Their migration would cease when the planet reached its final mass. Thus, this mechanism provides a natural way for a giant planet to pull in distant satellites without causing them to collide with the planet.

ACKNOWLEDGMENTS

REFERENCES

Arnold, V. I. (translated by K. Vogtmann and A. Weinstein) 1978. *Mathematical Methods of Classical Mechanics*, Springer-Verlag, New York.

Brown, E. W., and C. A. Shook 1964. *Planetary Theory*, Dover, New York.

Canup, R. M., and L. W. Esposito 1995. Accretion of the Moon from an impact-generated disk. *Icarus* **119**, 427–446.

Corben, H. C., and P. Stehle 1957. *Classical Mechanics*, Wiley, New York.

Danby, J. M. A. 1988. *Fundamentals of Celestial Mechanics*, Willmann-Bell, Richmond.

Duncan, M. J., and J. J. Lissauer 1998. The effects of post-main-sequence Solar mass loss on the stability of our planetary system. *Icarus* **134**, 303–310.

Duncan, M. J., H. F. Levison, and M. H. Lee 1998. A multiple step symplectic algorithm for integrating close encounters. *Astron. J.* **116**, 2067–2077.

Erdi, B. 1997. The Trojan problem. *Celest. Mech. Dynam. Astron.* **65**, 149–164.

Fernandez, J. A., and W. H. Ip 1996. Orbital expansion and resonant trapping during the late accretion stages of the outer planets. *Planet. Space Sci.* **44**, 431–439.

Gomes, R. S. 1997. Orbital evolution in resonance lock. I. The restricted 3-body problem *Astron. J.* **114**, 2166–2176.

Gomes, R. S. 1998. Dynamical effects of planetary migration on primordial Trojan-type asteroids. *Astron. J.* **116**, 2590–2597.

Hahn, J. M., and R. Malhotra 1999. Orbital evolution of planets embedded in a planetesimal disk. *Astron. J.* **117**, 3041–3053.

Heppenheimer, T. A., and C. Porco 1977. New contributions to the problem of capture. *Icarus* **30**, 385–401.

Horedt, G. P. 1974a. A variable mass of the primaries and librations around the triangular points. *Celest. Mech.* **10**, 319–326.

Horedt, G. P. 1974b. Mass loss in the plane circular restricted three-body problem: Application to the origin of the Trojans and of Pluto. *Icarus* **23**, 459–464.

Horedt, G. P. 1984. Trojan orbits with mass exchange of the primaries. *Celest. Mech.* **33**, 367–374.

Ida, S., R. M. Canup, and G. R. Stewart 1997. Lunar accretion from an impact-generated disk. *Nature* **389**, 353–357.

Jeans, J. H. 1961. *Astronomy and Cosmogony*, Dover, New York.

Kary, D. M., and J. J. Lissauer 1995. Nebular gas drag and planetary accretion II. Planet on an eccentric orbit. *Icarus* **117**, 1–24.

Landau, L. D., and E. M. Lifshitz 1960. *Mechanics*, Pergamon Press, NY.

Levison, H. F., E. M. Shoemaker, and C. S. Shoemaker 1997. Dynamical evolution of Jupiter's Trojan asteroids. *Nature* **385**, 42–44.

Marzari, F., and H. Scholl 1998. Capture of Trojans by a growing proto-Jupiter. *Icarus* **131**, 41–51.

Marzari, F., P. Farinella, D. R. Davis, H. Scholl, and A. Campo Bagatin 1997. Collisional evolution of Trojan asteroids. *Icarus* **125**, 39–49.

Morais, M. H. M. 1999. A secular theory for Trojan-type motion. *Astron. Astrophys.* **350**, 318–326.

Morais, M. H. M. 2000. *The effect of secular perturbations and mean motion resonances on Trojan dynamics*. Ph.D. dissertation, Queen Mary and Westfield College, London.

Murray, C. D. 1994. Dynamical effects of drag in the circular restricted three-body problem 1: Location and stability of the Lagrangian equilibrium points. *Icarus* **112**, 465–484.

Murray, C. D., and S. F. Dermott 1999. *Solar System Dynamics*, Cambridge Univ. Press, Cambridge.

Peale, S. J. 1993. The effect of the nebula on the Trojan precursors. *Icarus* **106**, 308–322.

Press, W. H., B. P. Flannery, S. A. Teukolsky, and W. T. Vettering 1987. *Numerical Recipes in C: The Art of Scientific Computing*, Cambridge Univ. Press, Cambridge.

Rabe, E. 1954. The Trojans as escaped satellites of Jupiter. *Astron. J.* **59**, 433–439.

Rabe, E. 1972. Orbital characteristics of comets passing through the 1:1 commensurability with Jupiter. In *Motion, Evolution of Orbits, and Origin of*

Comets. Proceedings, IAU Symposium No. 45 Leningrad (E. I. Chevotarev *et al.* Ed.), pp. 55–60. Springer-Verlag, New York/Berlin.

Shoemaker, E. M., C. S. Shoemaker, and R. F. Wolfe 1989. Trojan asteroids: Population, dynamical structure, and origin of the L4 and L5 swarms. In *Asteroids II* (R. P. Binzel, T. Gehrels, and M. S. Matthews, Eds.), pp. 487–523. Univ. of Arizona Press, Tucson.

Strömgren, E. 1903. Über die Bedeutung kleiner Massenänderungen für die Newtonsche Centralbewegung. *Astron. Nachr.* **163**, 129–136.

Ward, W. R. 1997. Survival of planetary systems *Astron. J. Lett.* **482**, 211–214.

Wisdom, J., and M. Holman 1991. Symplectic maps for the *n*-body problem. *Astron. J.* **102**, 1528–1538.

Yoder, C. F. 1979. Notes on the origin of the Trojan asteroids. *Icarus* **40**, 341–344.

Yoder, C. F., Colombo, G., Synnott, S. P., and K. A. Yoder 1983. Theory of motion of Saturn's coorbiting satellites. *Icarus* **53**, 431–443.